Royal Norwegian Council
for Scientific and Industrial Research
(NTNF)

NORSAR

NORSAR Scientific Report No. 2-87/88

Semiannual Technical Summary

1 October 1987 – 31 March 1988

L.B. Loughran (ed.)

Kjeller, June 1988

VII.7 Analysis of Gräfenberg Lg recordings of Semipalatinsk explosions

In the previous NORSAR Semiannual Technical Summary, it was demonstrated that Lg measurements from NORSAR recordings can provide very stable magnitude estimates for large underground nuclear explosions at the Semipalatinsk test site (Ringdal and Hokland, 1987).

In this paper, initial results are presented from a study of Gräfenberg Lg recordings, using the same estimation method as for NORSAR. At this stage, the main purpose has been to determine the degree of consistency that can be obtained between Lg measurements from two arrays, with a further aim being to extend the study to a network of stations and obtain additional improved stability through network averaging.

The Gräfenberg array (GRF) is located in southern Germany as shown on Fig. VII.7.1, where the propagation paths from Semipalatinsk to NORSAR and GRF are also indicated. The unique feature of the Gräfenberg array is that all data are recorded broadband, with an instrument response that is flat to velocity from about 20 second period to 5 Hz (Harjes and Seidl, 1978). Altogether, the array comprises 13 instrument sites, of which three are 3-component systems (Fig. VII.7.2).

The data base used for this initial study comprised GRF recordings of 58 Semipalatinsk explosions between 1976 and 1987. Of the 58 events, 39 were sufficiently large to produce Lg wave amplitudes significantly exceeding the background noise level in the frequency band 0.6-3.0 Hz, and these are listed in Table VII.7.1. Specifically, we required that the RMS Lg should be at least 1.5 times the RMS of noise preceding P in this selection process. We also deleted from further analysis three events which had interfering phases in the Lg time window.

Data analysis was carried out using the same procedure as described by Ringdal and Hokland (1987). Briefly, all channels were filtered using a

Butterworth 3rd order recursive bandpass filter (0.6 - 3.0 Hz), and RMS values were then computed from a 60-second noise window (starting 80 seconds before P onset) and for a 120-second Lg window (starting 14 minutes after P onset). A noise compensation procedure was then carried out (as in the paper cited above), and a constant correction was applied to obtain the GRF Lg magnitudes. This constant was determined by requiring that the average GRF Lg magnitudes should equal the average NORSAR Lg magnitudes for the common event set.

The resulting magnitudes are listed in Table VII.7.1. These data are based only on the instruments A1, A2, A3 and A4 (vertical components), since our data base for the earliest events did not comprise recordings from all 13 channels. (We considered it important to use the same instruments for the entire data base, in order to avoid possible bias effects due to local receiver anomalies.)

Fig. VII.7.3 gives a comparison of Lg magnitudes determined from Gräfenberg and NORSAR data. The consistency between these estimates is excellent, with the standard deviation of the differences being only 0.051 magnitude units. If we consider only well-recorded events at GRF, i.e., requiring at least 3 stations and signal-to-noise ratio (RMS Lg to RMS noise) of at least 1.75, the standard deviation is reduced even further, to 0.043 magnitude units (Fig. VII.7.4).

It appears from the two figures that the GRF Lg magnitudes tend to be slightly higher than NORSAR Lg magnitudes for the largest events. It must be noted here that the estimates are less accurate for the smaller events, due to greater noise interference, but it is also possible that the differences in instrument responses at GRF and NORSAR could be a contributing factor. In this initial study, we have not attempted to compensate for this response difference, although this is certainly a natural next step.

Fig. VII.7.5 shows P-Lg (GRF) magnitude residuals on the basis of geographical epicenter location within the Shagan River area. The location estimates and maximum likelihood ISC-based magnitudes used for generating this figure have been obtained from Blacknest (Marshall et al, 1985; Marshall, personal communication). We note the systematic difference between the northeast and southwest portion of the test site; in fact this pattern is almost identical to that found using NORSAR Lg data (Ringdal and Hokland, 1987). The fact that this anomaly is confirmed using an entirely different array for Lg measurements is by itself significant, as it demonstrates that this observation is not a function of the particular propagation path from Semipalatinsk to NORSAR.

Conclusions

From this initial study, we can conclude that the Lg RMS estimation methods provide very stable, mutually consistent results when applied to two widely separated arrays (NORSAR and GRF). This is of clear significance regarding the potential use of such Lg measurements for yield estimation. Further research will be directed toward expanding the data base and number of instruments in the Gräfenberg study, including addressing the instrument response issue, and in addition conduct similar studies using other available station data as well as study Lg recordings from other test sites.

F. Ringdal
J. Fyen

References

Harjes, H.-P. and D. Seidl (1978): Digital recording and analysis of broadband seismic data at the Gräfenberg (GRF) array. J. Geophys. Res., 44, 511-523.

Marshall, P.D., T.C. Bache and R.C. Lilwall (1985): Body wave magnitudes and locations of Soviet underground explosions at the Semipalatinsk Test Site. AWRE Report No. O 16/84, AWRE, MOD(PE), Aldermaston, Berksh., UK.

Ringdal, F. and B.Kr. Hokland (1987): Magnitudes of large Semipalatinsk explosions using P coda and Lg measurements at NORSAR. Semiannual Technical Summary, 1 Apr - 30 Sep 1987, NORSAR Sci. Rep. No. 1-87/88, Kjeller, Norway.

ORIGIN DATE	ORIGIN TIME	GRF LG RMS	NCH
04/07/76-186	02.56.57.60	5.781	04/04
28/08/76-241	02.56.57.50	5.673	03/04
23/11/76-328	05.02.57.28	5.811	03/03
07/12/76-342	04.56.57.38	5.721	03/03
29/05/77-149	02.56.57.80	5.592	03/03
11/06/78-162	02.56.57.70	5.748	02/06
29/08/78-241	02.37.06.50	6.005	03/07
04/11/78-308	05.05.57.50	5.640	03/06
29/11/78-333	04.32.58.00	5.894	01/06
23/06/79-174	02.56.57.60	6.101	03/06
07/07/79-188	03.46.57.40	5.926	04/10
04/08/79-216	03.56.57.60	6.093	04/12
18/08/79-230	02.51.57.30	6.144	04/10
28/10/79-301	03.16.56.90	6.062*	00/10
02/12/79-336	04.36.57.50	5.955	04/12
23/12/79-357	04.56.57.60	6.058	04/09
29/06/80-181	02.32.57.70	5.699	03/13
12/10/80-286	03.34.14.10	5.954	04/13
14/12/80-349	03.47.06.60	5.946	02/13
27/12/80-362	04.09.08.20	5.866	03/13
22/04/81-112	01.17.11.40	5.967	03/13
13/09/81-256	02.17.18.25	6.081	04/09
18/10/81-291	03.57.02.64	5.945	04/09
27/12/81-361	03.43.14.10	6.114	03/11
05/12/82-339	03.37.12.60	5.995	04/13
26/12/82-360	03.35.14.10	5.603	04/13
07/03/84-067	02.39.06.40	5.556	04/13
29/03/84-089	05.19.08.20	5.948	04/13
26/05/84-147	03.13.12.40	6.109	04/13
02/12/84-337	03.19.06.30	5.842	04/13
03/04/87-093	01.17.08.00	6.129	04/13
17/04/87-107	01.03.04.00	5.912	04/13
06/05/87-126	04.02.05.50	5.883	04/13
20/06/87-171	00.53.04.00	5.947	03/13
17/07/87-198	01.17.07.00	5.686	04/13
02/08/87-214	00.58.08.00	5.835	04/13
15/11/87-319	03.31.08.00	6.006	04/13
13/12/87-347	03.21.08.00	6.066	04/13
27/12/87-361	03.05.08.00	6.044	04/13

Table VII.7.1 List of events used in this study, with estimated Lg magnitudes from Gräfenberg recordings as described in the text. The number of A-ring GRF channels used for these measurements are also given, together with the total number of GRF channels available in the data base. For the event marked with an asterisk, the estimate is based on GRF B-ring data.

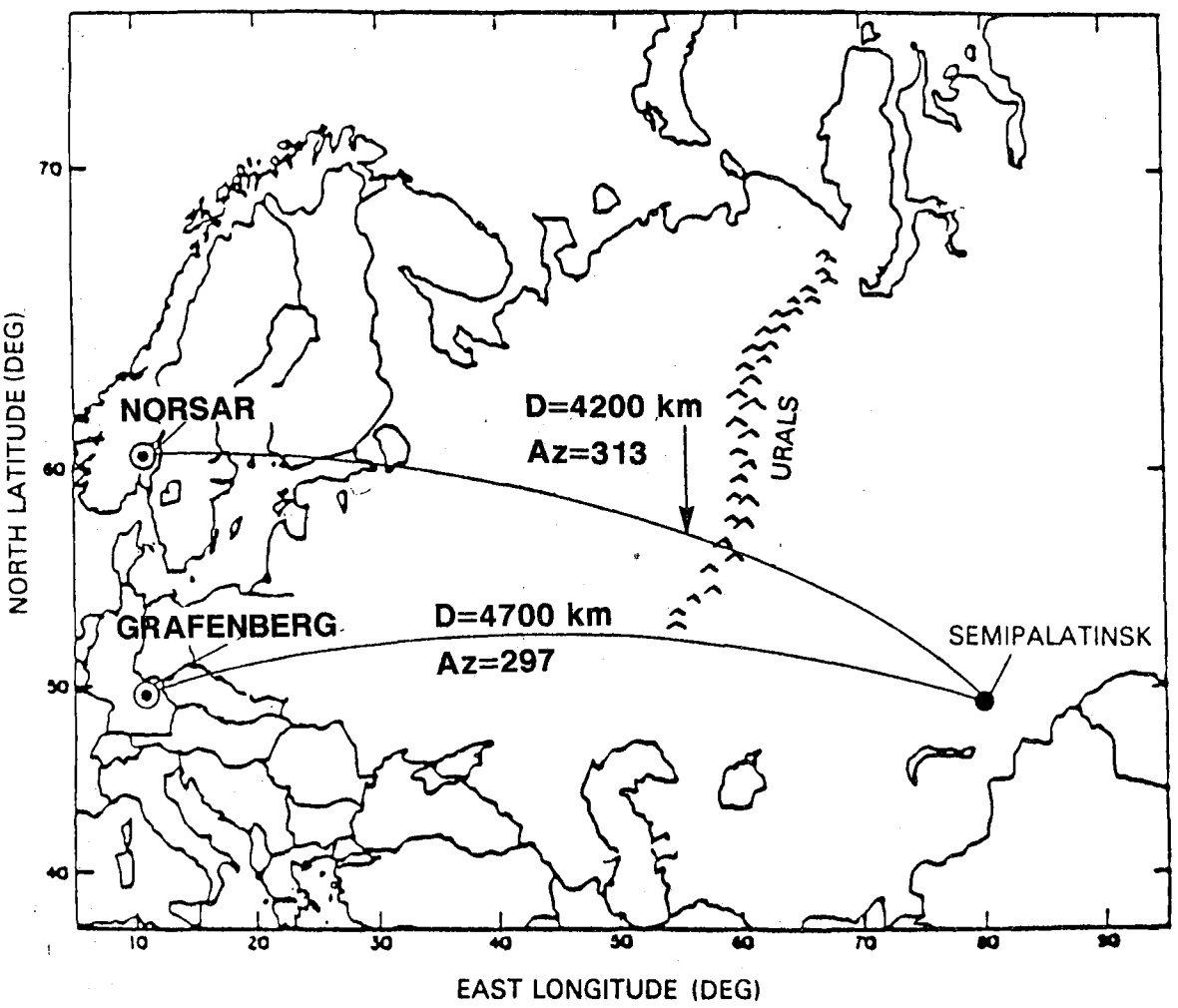

Fig. VII.7.1 Location of the NORSAR and Gräfenberg arrays in relation to the Semipalatinsk test site.

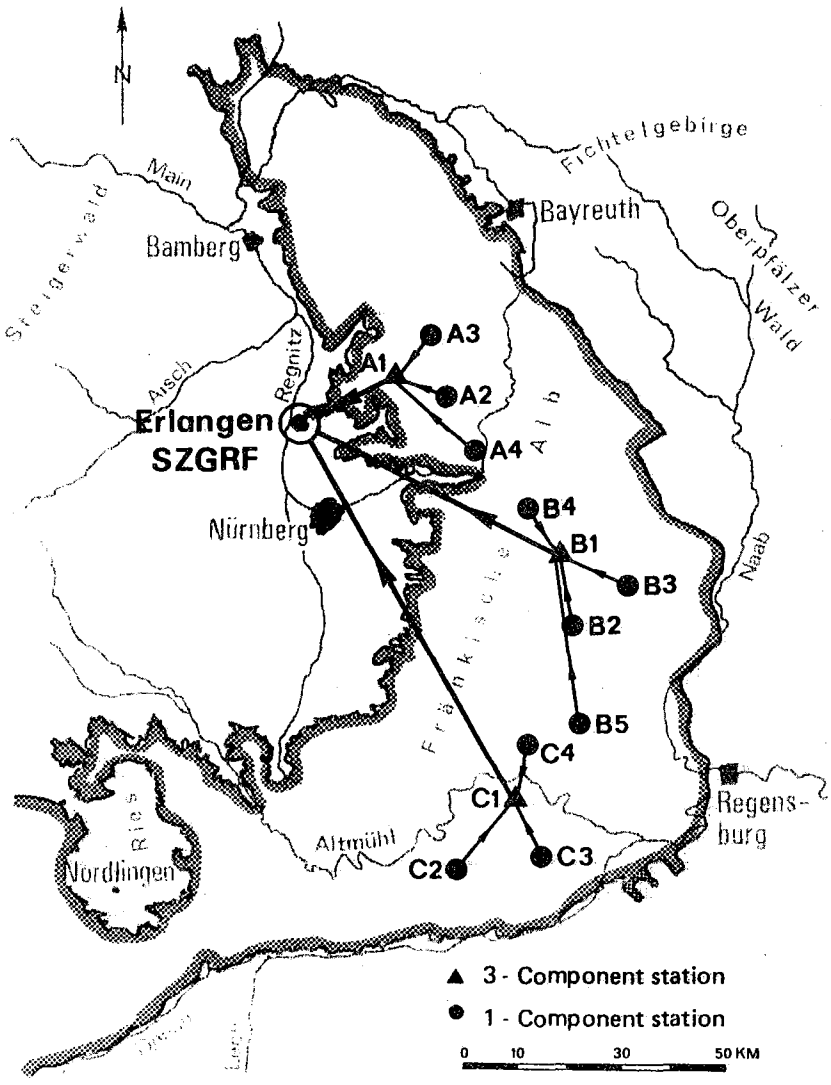

Fig. VII.7.2 Geometry of the Gräfenberg array.

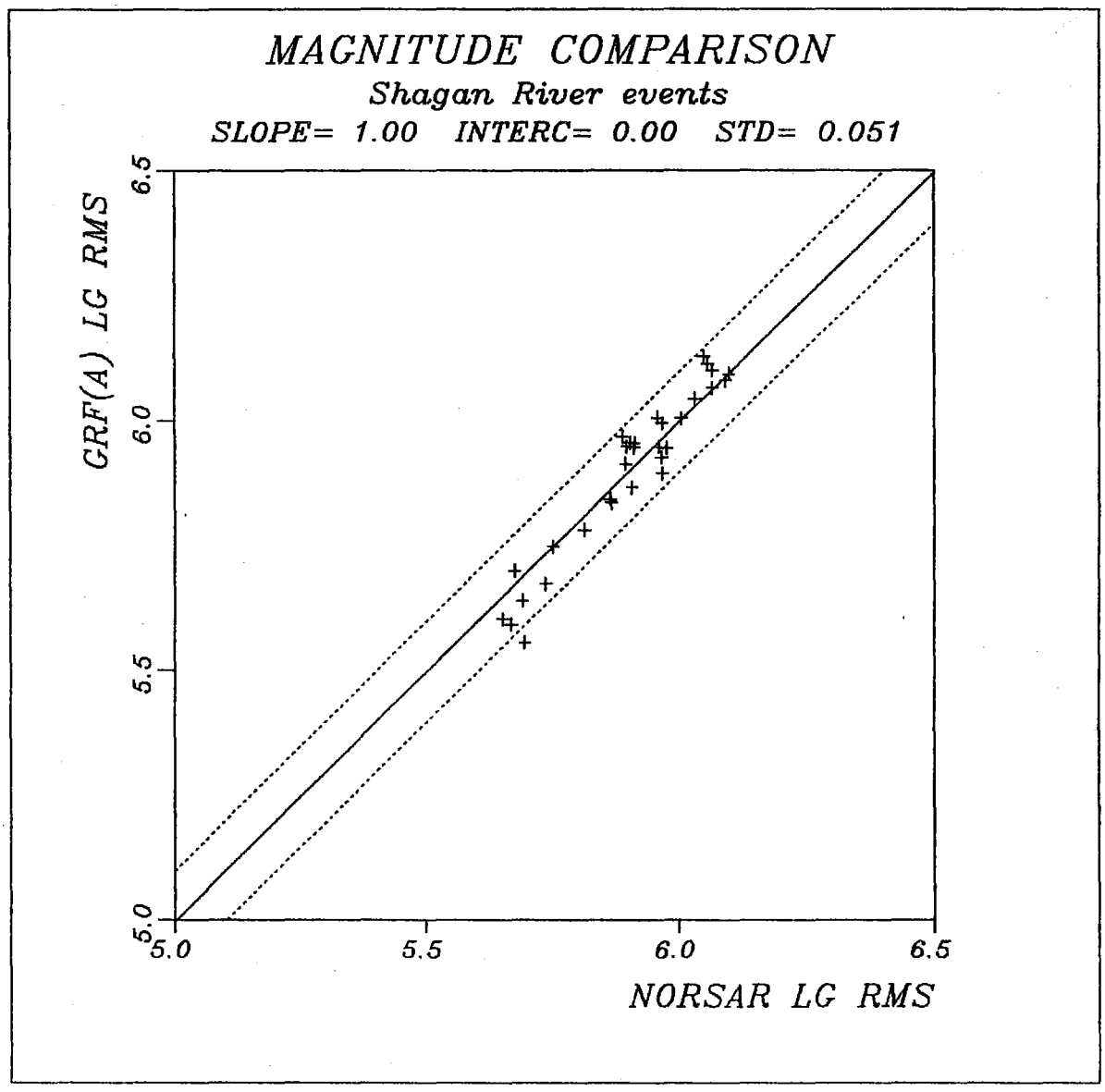

Fig. VII.7.3 Plot of Gräfenberg versus NORSAR Lg magnitudes for Semipalatinsk explosions. The slope has been restricted to 1.00, and the dotted lines correspond to plus/minus two standard deviations.

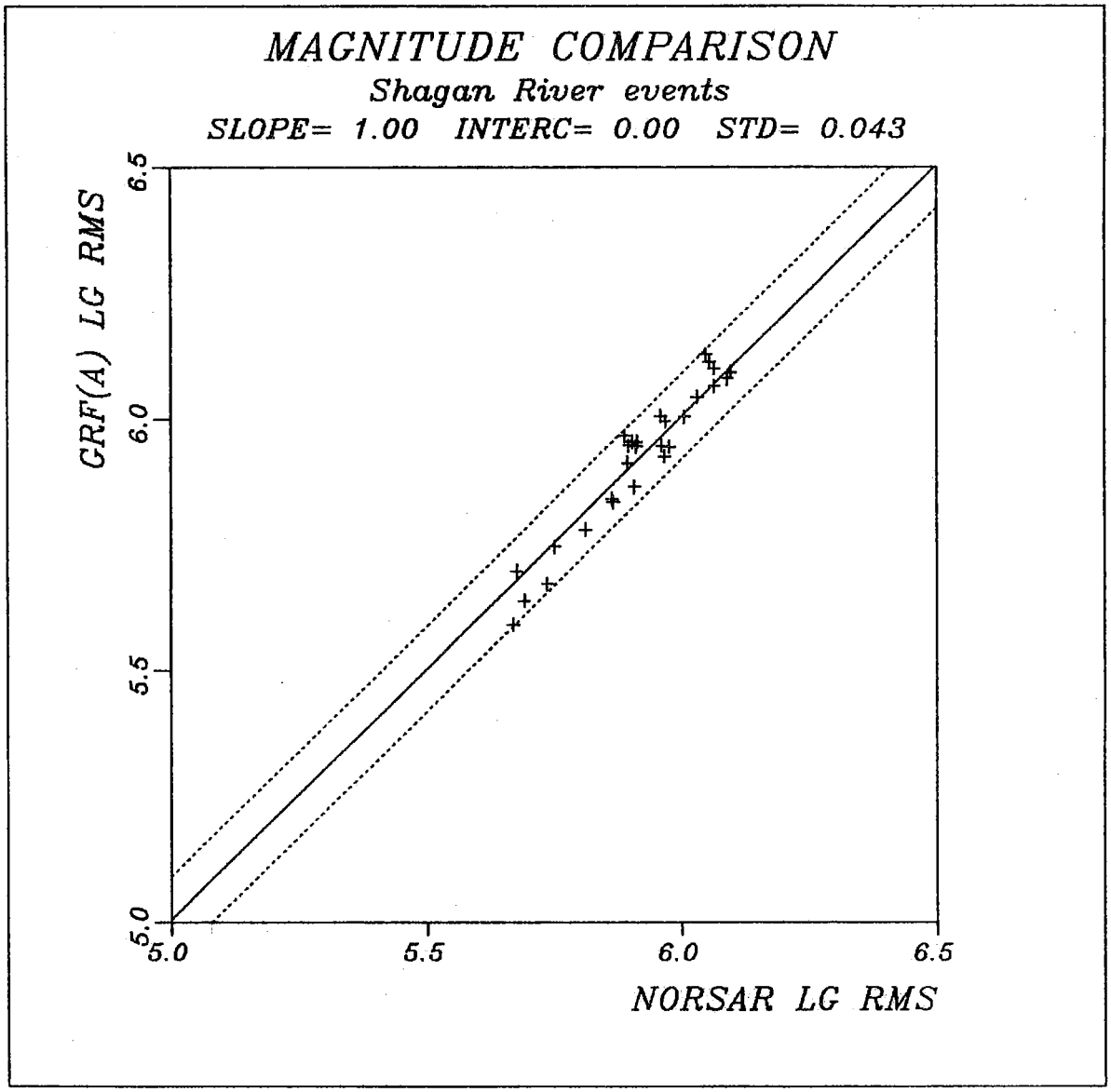

Fig. VII.7.4 Same as Fig. VII.7.3, but including only events with GRF Lg measurements based on at least three channels, and having signal-to-noise ratio exceeding 1.75 (see text for details). Note that the scatter is considerably reduced compared to Fig. VII.7.3.

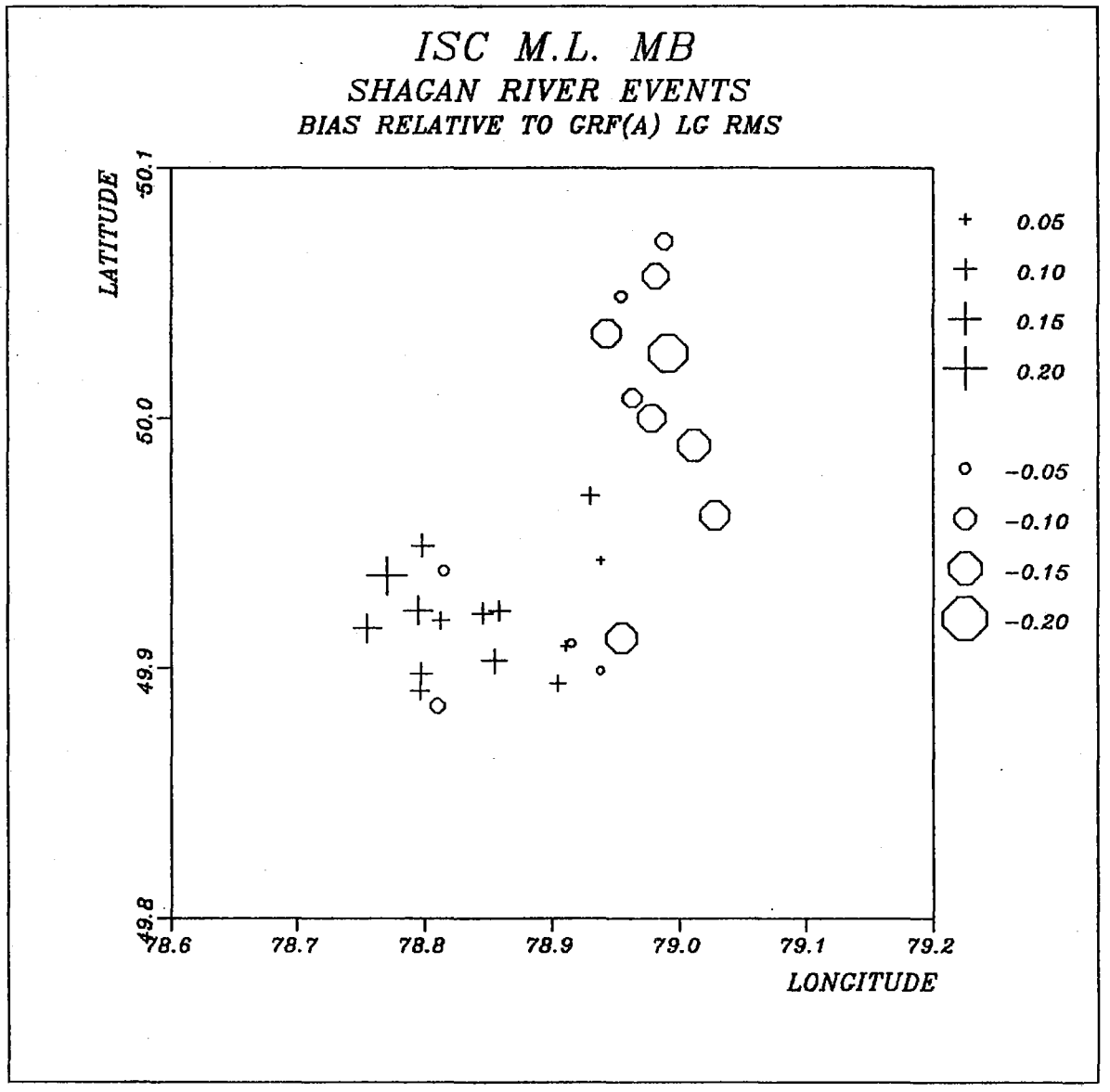

Fig. VII.7.5 Plot of magnitude residuals (ISC max. likelihood m_b minus Gräfenberg Lg RMS magnitudes) as a function of event location for events in the data base. Plusses and circles correspond to residuals greater or less than the average, respectively, with symbol size proportional to the deviation. Location estimates are those of Marshall et al (1985) where available, otherwise NEIS estimates have been used. Note the systematic variation within the Shagan River area.